Uplink Capacity and Interference Avoidance for Two-Tier Femtocell Networks

Vikram Chandrasekhar and Jeffrey G. Andrews

Abstract

Two-tier femtocell networks– comprising a conventional macrocellular network plus embedded femtocell hotspots– offer an economically viable solution to achieving high cellular user capacity and improved coverage. With universal frequency reuse and DS-CDMA transmission however, the ensuing cross-tier cochannel interference (CCI) causes unacceptable outage probability. This paper develops an uplink capacity analysis and interference avoidance strategy in such a two-tier CDMA network. We evaluate a network-wide area spectral efficiency metric called the *operating contour (OC)* defined as the feasible combinations of the average number of active macrocell users and femtocell base stations (BS) per cell-site that satisfy a target outage constraint. The capacity analysis provides an accurate characterization of the uplink outage probability, accounting for power control, path-loss and shadowing effects. Considering worst case CCI at a corner femtocell, results reveal that interference avoidance through a time-hopped CDMA physical layer and sectorized antennas allows about a 7x higher femtocell density, relative to a split spectrum two-tier network with omnidirectional femtocell antennas. A femtocell exclusion region and a tier selection based handoff policy offers modest improvements in the OCs. These results provide guidelines for the design of robust shared spectrum two-tier networks.

Index Terms

Operating Contours, CDMA, Macrocell, Femtocell, Cellular, Uplink Capacity, Outage Probability

I. Introduction

Two-tier femtocell networks are in the process of being deployed to improve cellular capacity [1], [2]. A femtocell serves as a small range data access point situated around high user density

Affiliated with the Wireless Networking and Communications Group, Dept. of Electrical and Computer Engineering at the University of Texas at Austin. Email:cvikram@mail.utexas.edu,jandrews@ece.utexas.edu, Date: September 10, 2018.

hot-spots serving stationary or low-mobility users. Examples of femtocells include residential areas with home LAN access points, which are deployed by end users and urban hot-spot data access points. A femtocell is modeled as consisting of a randomly distributed population of actively transmitting users. The femtocell radio range ($10-50$ meters) is much smaller than the macrocell radius ($300-2000$ meters) [3]. Users transmitting to femtocells experience superior signal reception and lower their transmit power, consequently prolonging battery life. The implication is that femtocell users cause less CCI to neighboring femtocells and other macrocell users. Additionally, a two-tier network offsets the burden on the macrocell BS, provided femtocells are judiciously placed in traffic hot-spots, improving network capacity and QoS.

Observe that it is easier to implement a two-tier network by sharing spectrum from an infrastructural perspective, as the protocol does not require the mobile to implement spectrum searching, which is energy inefficient. The focus of this work is to answer the following questions:

- What is the two-tier uplink capacity in a typical macrocell with randomly scattered hotspots, assuming a randomly distributed population of actively transmitting users per femtocell?
- Is it possible to accurately characterize the statistics of the cross-tier CCI? What is the effect of the femtocell hotspot density, macrocell-femtocell power ratio and femtocell size?
- How much benefit is accrued by interference avoidance using antenna sectoring and time hopping in CDMA transmission? What is the impact of using a femtocell exclusion region and a tier selection policy for femtocell handoff?

By addressing these questions, our work augments existing research on capacity analysis and CCI mitigation in two-tier networks. We show that creating a suitable infrastructure for curbing cross-tier CCI can actually increase the uplink capacity for a shared spectrum network.

A. *Related work*

From a physical layer viewpoint, prior research has mainly focused on analyzing the uplink capacity, assuming either a single microcell[1] or multiple regularly spaced microcells in a macro-cell site. This model has assumed significance for its analytical tractability, nonetheless, it has limited applicability owing to the inherent variability in microcell locations in realistic scenarios.

[1]In the context of this paper, a microcell has a much larger radio range (100-500 m) than a femtocell.

The ideas presented in this paper are most closely related to the work by Kishore *et al.* The downlink cellular capacity of a two-tier network is derived in [4]. The results show that the cellular user capacity is limited by uplink performance for both slow and fast power control. In [5], the OCs for a two-tier network are derived for different tier-selection schemes, assuming an arbitrarily placed microcell. Further work by the same author [6], [7] extended the framework to multiple microcells embedded inside multiple macrocells. The cross-tier CCI is approximated by its average and cross-tier microcell to microcell CCI is ignored. The resulting analysis is shown to be accurate only up to 8 microcells per macrocell. Our results, on the other hand, are accurate over a wide range of femtocell densities, without approximating the CCI statistics.

Related work includes [8], which discusses the benefits of having a tilted antenna radiation pattern and macrocell-microcell power ratio control. In [9], [10], a regular network comprising a large hexagonal macrocell and smaller hexagonal microcells is considered. Citing near far effects, the authors conclude that it is more practical to split the RF spectrum between each tier. The reason being that the loss in trunking efficiency by splitting the spectrum is lower than the increase in outage probability in a shared spectrum two-tier network. Our paper, in contrast, shows a higher user capacity for a shared spectrum network by enforcing *higher spatial reuse* through small femtocells and *interference avoidance* by way of antenna sectoring and Time hopped CDMA (TH-CDMA) in each tier.

Finally, from a network perspective, Joseph *et al.* [11] study impact of user behavior, load balancing and different pricing schemes for interoperability between Wi-Fi hotspots and cellular networks. In [3], the design of a multitiered wireless network with Poisson call arrivals is formulated as an constrained optimization problem, and the results highlight the economic benefits of a two-tier network infrastructure: increased stability in system cost and a more gradual performance degradation as users are added.

B. Contributions

This paper employs a stochastic geometry framework for modeling the *random* spatial distribution of users/femtocells, in contrast to prior work [5]–[7], [9], [10], [12]. Hotspot locations are likely to vary from one cellsite to another, and be opportunistic rather than planned: Therefore a capacity analysis that embraces instead of neglecting randomness will naturally provide more accurate results and more plausible insights.

To model the user/hotspot locations, the paper assumes that the macrocell users and femtocell BS are randomly distributed as a Homogeneous Spatial Poisson Point Process (SPPP). The Poisson process is a natural model arising from mobility of macrocellular users and placement of femtocell BS in densely populated areas [13], and has been confirmed in empirical studies and used in prior work. For example, Chan and Hanly [14] have used the Poisson model for describing the out-of-cell interference in a CDMA cellular network. The three key contributions in our paper can be summarized as:

- First, a novel outage probability analysis is presented, accounting for *cellular geometry*, *cross-tier CCI* and *shadowing* effects. We derive tight lower bounds on statistics of macrocell CCI at any femtocell hotspot BS along the hexagonal axis. Next, assuming small femtocell sizes, a Poisson-Gaussian model for macrocell CCI and alpha-stable distribution for cross-tier femtocell CCI is shown to accurately capture the statistics at the macrocell BS. In the analysis, outage events are explicitly modeled rather than considering average interference as in [9], [12]. For doing so, the properties of Poisson shot-noise processes (SNP) [15], [16] and Poisson void probabilities [17] are used for deriving the uplink outage probabilities.
- Second, robust interference avoidance is shown to enable two-tier networks with universal frequency reuse to achieve higher user capacity, thereby avoiding the design of protocols which require the mobile to sense the spectrum. With interference avoidance, an equitable distribution of users between tier 1 and tier 2 networks is shown to be achieved with an *order-wise difference* in the ratio of their received powers. Even considering the worst case cross-tier CCI at a corner femtocell, results for moderately loaded macrocellular networks reveal that interference avoidance provides a *7x increase* in femtocell BS density over split spectrum two-tier networks.
- Third, additional interference avoidance using a combination of femtocell exclusion and tier selection based femtocell handoff offers modest improvements in the network OCs. This suggests that at least for small femtocell sizes, time hopping and antenna sectoring offer the largest gains in user capacity for shared spectrum two-tier networks.

II. System Model

Denote $\mathcal{H} \subset \mathbb{R}^2$ as the interior of a reference hexagonal macrocell C (Fig. 1) of radius R_c. The tier 1 network consists of low density macrocellular users that are communicating with the central BS in each cellsite. The macrocellular users are distributed on $\mathbb{R}^2$ according to a homogeneous SPPP Ω_c of intensity λ_c. The overlaid tier 2 network containing the femtocell BS's forms a homogeneous SPPP[2] Ω_f with intensity λ_f. Each femtocell hotspot includes a Poisson distributed population of actively transmitting users[3] with mean U_f in a circular coverage area of radius $R_f, R_f \ll R_c$. To maximize user capacity per cellsite, it is desirable to have $\lambda_f \gg \lambda_c$; as will be shown, cross-tier CCI at a macrocell BS limits λ_f for a given λ_c. Defining $|\mathcal{H}| \triangleq 2.6R_c^2$ as the area of the hexagonal region $\mathcal{H}$, the mean number of macrocell users and femtocell BS's per cellsite are given as $N_c = \lambda_c \cdot |\mathcal{H}|$ and $N_f = \lambda_f \cdot |\mathcal{H}|$ respectively. Table I shows a summary of important parameters and typical values for them, which are used later in numerical simulations.

Users in each tier employ DS-CDMA with processing gain G. Uplink power control adjusts for propagation losses and log-normal shadowing, which is standard in contemporary CDMA networks. The macrocell and femtocell receive powers are denoted as P_r^c and P_r^f respectively. Any power control errors [18] and short-term fading effects are ignored for analytical convenience. We affirm this assumption as reasonable, especially in a wideband system with significant frequency diversity and robust reception (through RAKE receiver, coding and interleaving).

A. TH-CDMA and Antenna sectoring

Suppose that the CDMA period $T = G \cdot T_c$ is divided into N_{hop} hopping slots, each of duration T/N_{hop}. Every macrocell user and femtocell (all active users within a femtocell transmit in the same hopping slot) independently choose to transmit over any one slot, and remain silent over the remaining $N_{hop} - 1$ slots. The resulting intra- and cross-tier interference are "thinned" by a factor of N_{hop} [17]. Using TH-CDMA, users in each tier effectively sacrifice a factor N_{hop} of their processing gain, but benefit by thinning the interfering field by the same factor.

We further assume sectored antenna reception (Fig. 2) in both the macrocell and femtocell BS, with antenna alignment angle θ and sector width equaling $2\pi/N_{sec}$. While antenna sectoring is a common feature at the macrocell BS in practical cellular systems, this paper proposes to use sectored antennas at femtocell BS's as well. The reason is that the cross-tier CCI caused by nearby macrocellular users can lead to unacceptable outage performance over the femtocell uplink; this motivates the need for directed femtocell antennas. The spatial thinning effect of TH-CDMA transmission and antenna sectoring is analytically derived in the following lemma.

[2]The system model allows a macrocellular user to be present inside a femtocell as the governing process Ω_c is homogeneous.

[3]A hard handoff is assumed to allocate subscribed hotspot users to a femtocell, provided they fall within its radio range.

Lemma 1 (Spatial thinning by interference avoidance): With TH-CDMA transmission over N_{hop} slots and antenna sectoring with N_{sec} directed BS antennas in each tier, the interfering field at a given BS antenna sector can be mapped to the SPPPs Φ_c and Φ_f on $\mathbb{R}^2$ with intensities $\eta_c = \lambda_c/(N_{hop} \cdot N_{sec})$ and $\eta_f = \lambda_f(1 - e^{-U_f})/(N_{hop} \cdot N_{sec})$ respectively.

Proof: See Appendix I. ■

The following definitions will be useful in the remainder of the paper.

Definition 1: Denote $\mathcal{H}_{sec} \subseteq \mathcal{H}$ as the region within $\mathcal{H}$ covered by a BS antenna sector corresponding to a macrocell BS or a femtocell BS within the reference cellsite. For example, $\mathcal{H}_{sec} = \mathcal{H}$ for an omnidirectional femtocell located at the corner of the reference macrocell.

Definition 2: Denote $\hat{\Omega}_c$ and $\hat{\Omega}_f$ as the heterogeneous SPPPs composed of active macrocell and femtocell interferers as seen at a BS antenna sector in each tier, whose intensities are given by $\hat{\lambda}_c$ and $\hat{\lambda}_f$ in (11). Denote the equivalent mapped homogeneous SPPPs over $\mathbb{R}^2$ by Φ_c and Φ_f whose intensities are given by η_c and η_f respectively.

Definition 3: Denote the restriction of $\hat{\Omega}_c$ and $\hat{\Omega}_f$ to $\mathcal{H}$ by the SPPPs Π_c and Π_f respectively.

B. Channel Model and Interference

The channel is represented as a combination of path-loss and log-normal shadowing. The path-loss exponents are denoted by α (outdoor transmission) and β (indoor femtocell transmission) while lognormal shadowing is parameterized by its standard deviation σ_{dB}.

Through uplink power control, a macrocell user transmitting at a random position X w.r.t the reference macrocell BS C chooses a transmit power level $P_t^c = P_r^c/g_c(|X|)$. Here $g_c(|X|)$ is the attenuation function defined as $g_c(|X|) = K_c(d_{0c}/|X|)^\alpha \Theta_C$ where $10\log_{10}\Theta_C \sim \mathcal{N}(0, \sigma_{dB}^2)$ is the log-normal shadowing from user to C, $K_c \triangleq [c/(4\pi f_c d_{0c})]^2$ is a unitless constant that depends on the wavelength of the RF carrier c/f_c and outdoor reference distance d_{0c}. Similarly, a femtocell user at a random position Y within a femtocell BS F chooses a transmit power $P_t^f = P_r^f/g_f(|Y|)$, where $g_f(|Y|) = K_f(d_{0f}/|Y|)^\beta \Theta_F$, $10\log_{10}\Theta_F \sim \mathcal{N}(0, \sigma_{dB}^2)$ and $K_f \triangleq [c/(4\pi f_c d_{0f})]^2$. Here d_{0f} is the reference distance for calculating the indoor propagation loss. Note that in reality, K_c and K_f are empirically determined. The interference in each tier (Fig. 2) can be grouped as:

Macrocell interference at a macrocell BS ($I_{c,in}, I_{c,out}$): Through power control, all macrocell users within $\mathcal{H}_{sec}$ are received with constant power P_r^c, so the in-cell interference equals $(N-1) \cdot P_r^c$, where $N \sim \text{Poisson}(N_c/N_{hop})$. As such, inferring the exact statistics of out-of-cell macrocellular interference $I_{c,out}$ is analytically intractable; it is assumed that $I_{c,out}$ is distributed according to a scaled Gaussian pdf [14]. Defining μ and σ^2 to be the empirically determined parameters of the Gaussian, the pdf of $I_{c,out}$ is given as $f_{I_{c,out}}(y) = \frac{2e^{-\frac{1}{2}(y-\mu)^2/\sigma^2}}{\sqrt{2\pi\sigma^2}[2-\text{erfc}(\frac{\mu}{\sqrt{2}\sigma})]}$, where $\text{erfc}(t) \triangleq \sqrt{\frac{2}{\pi}} \int_{t\sqrt{2}}^{\infty} e^{-x^2/2} dx$.

Femtocell interference at a macrocell BS ($I_{c,f}$) : Say femtocell F_i with $U_i \sim \text{Poisson}(U_f)$ users is located at random position X_i w.r.t reference macrocell BS C. Inside F_i, a randomly placed Tier 2 user j at distance Y_j from the femtocell BS transmits with power $P_t^f(j) = P_r^f / g_f(Y_j)$. The interference caused at C from user j inside F_i is given as,

$$I_{c,f}(F_i, j) = P_r^f g_c(|X_i + Y_j|)/g_f(|Y_j|) \approx P_r^f g_c(|X_i|)/g_f(R_f) = Q_f \Theta_{j,C}/\Theta_{j,F_i} |X_i|^{-\alpha} \quad (1)$$

where $Q_f \triangleq P_r^f R_f^{\beta} \frac{K_c d_{0c}^{\alpha}}{K_f d_{0f}^{\beta}}$. In doing so, we make two important assumptions:

***AS** 1:* For small sized femtocells ($R_f \ll R_c$), a femtocell or macrocell BS sees CCI from other femtocells as a *point source* of interference, implying $g_c(|X_i + Y_j|) \approx g_c(|X_i|)$.

***AS** 2:* When analyzing the interference caused by a random femtocell F_i at any other location, the U_i femtocell users can be modeled as transmitting with maximum power, so that $g_f(|Y_j|) \approx g_f(R_f)$. This is for analytical tractability and modeling worst-case interference.

Summing (1) over all femtocells over a antenna sector at a macrocell BS, the cumulative cross-tier CCI at the reference macrocell BS C is represented by the Poisson SNP [15],

$$I_{c,f} = \sum_{F_i \in \hat{\Omega}_f} Q_f \Psi_i |X_i|^{-\alpha} \quad (2)$$

where $\Psi_i \triangleq \sum_{l=1}^{U_i} \Theta_{l,C}/\Theta_{l,F_i}$ defines the cumulative shadowing gain between actively transmitting users in femtocell F_i and macrocell BS C.

Neighboring femtocell interference at a femtocell BS ($I_{f,f}$) : By an identical argument as above, the interference caused at BS antenna sector of femtocell F_j from other femtocells $F_i, i \neq j$ is a Poisson SNP given by $I_{f,f} = \sum_{F_i \in \hat{\Omega}_f} Q_f \Psi_i |X_i|^{-\alpha}$, where $|X_i|$ refers to the distance between (F_i, F_j) and $\Psi_i \triangleq \sum_{l=1}^{U} \Theta_{l,F_j}/\Theta_{l,F_i}$.

Interference from active users within a femtocell ($I_{f,in}$) : Conditioned on the femtocell containing $U \geq 1$ actively transmitting users, the intra-tier CCI experienced by the user of interest arising from simultaneous transmissions within the femtocell equals $(U-1) \cdot P_r^f, \mathbb{E}[U] = \frac{U_f}{1-e^{-U_f}}$.

Macrocell interference at a femtocell BS ($I_{f,c}$) : This paper analyzes outage probability at a femtocell BS F_j located on the hexagonal axis, considering the effect of in-cell macrocellular CCI. The interference $I_{f,c}^{lb}$ arising from users in Π_c forms a lower bound on the cumulative tier 1 CCI $I_{f,c}$ and represented as $I_{f,c} \geq I_{f,c}^{lb} = \sum_{i \in \Pi_c} P_r^c \Psi_i (\frac{|X_i|}{|Y_i|})^\alpha$, where $\Psi_i \triangleq \Theta_{i,F_j}/\Theta_{i,C}, 10\log_{10}\Psi_i \sim \mathcal{N}(0, 2\sigma_{dB}^2)$ is the LN shadowing term and $|X_i|, |Y_i|$ represent the distances of macrocell user i to the macrocell BS and femtocell BS respectively. Observe that a corner femtocell experiences a significantly higher macrocell CCI relative to an interior femtocell, therefore the cdf $F_{I_{f,c}}(\cdot)$ is not a stationary distribution.

III. Per Tier Outage Probability

To derive the OCs, an uplink outage probability constraint is formulated in each tier. Define N_f and N_c as the average number of femtocell BS's and macrocell users per cellsite respectively. A user experiences outage if the received instantaneous Signal-to-Interference Ratio (SIR) over a transmission is below a threshold γ. Any feasible $(\tilde{N}_f, \tilde{N}_c)$ satisfies the outage probability requirements $\mathbb{P}_{out}^f \leq \epsilon, \mathbb{P}_{out}^c \leq \epsilon$ in each tier. The outage probabilities $\mathbb{P}_{out}^c(N_f, N_c)$ [resp. $\mathbb{P}_{out}^f(N_f, N_c)$] are defined as the probabilities that the despread narrowband SIR for a macrocell user [femtocell user] at the Tier 1 [Tier 2] BS antenna sector is below γ. Assuming the PN code cross-correlation equals N_{hop}/G[4], define

$$\mathbb{P}_{out}^c(N_f, N_c) = \Pr\left(\frac{G/N_{hop}P_r^c}{I_{c,in} + I_{c,out} + I_{c,f}} \leq \gamma \middle| |\hat{\Omega}_c| \geq 1\right)$$
$$\mathbb{P}_{out}^f(N_f, N_c) = \Pr\left(\frac{G/N_{hop}P_r^f}{(U-1)\cdot P_r^f + I_{f,f} + I_{f,c}} \leq \gamma \middle| U \geq 1\right) \quad (3)$$

where $|\hat{\Omega}_c|$ denotes the number of points in $\hat{\Omega}$ and the unconditioned $U \sim \mathrm{Poisson}(U_f/N_{sec})$. The OCs for the macrocell [resp. femtocell] are obtained by computing the *highest* N_f [N_c] for a given N_c [N_f], which satisfy a target outage constraint ϵ. More formally,

$$\tilde{N}_f(N_c) = \sup\{N_f : \mathbb{P}_{out}^c(N_f, N_c) \leq \epsilon\}, \tilde{N}_c(N_f) = \sup\{N_c : \mathbb{P}_{out}^f(N_f, N_c) \leq \epsilon\} \quad (4)$$

The OCs for the two-tier network are obtained corresponding to those feasible combinations of $(\tilde{N}_c, \tilde{N}_f)$ that *simultaneously* satisfy $\mathbb{P}_{out}^f \leq \epsilon$ and $\mathbb{P}_{out}^c \leq \epsilon$ respectively. For doing so, we derive the following theorems which quantify the outage probabilities and CCI statistics in each tier.

[4]With $N_{hop} = G = 1$, the model reduces to a non CDMA narrowband transmission; with $N_{hop} = G \gg 1$, the model reduces to a timeslotted ALOHA channel

Theorem 1: For small femtocell sizes, the statistics of the cross-tier femtocell CCI $I_{c,f}$ *(and intra-tier femtocell CCI* $I_{f,f}$*) at a BS antenna sector are given by a Poisson SNP* $Y = \sum_{i \in \Phi_f} Q_f \Psi_i |X_i|^{-\alpha}$ *with iid* $\Psi_i = \sum_{j=1}^{U_i} \Psi_{ij}, 10\log_{10}\Psi_{ij} \sim \mathcal{N}(0, \sigma_{dB}^2), U_i \sim U|U \geq 1$ *and* $U \sim \text{Poisson}(U_f)$. *In particular, if the outdoor path-loss exponent* $\alpha = 4$, *then* Y *follows a Lévy-stable distribution with stability exponent* $1/2$, *whose pdf and cdf are given as:*

$$f_Y(y) = \sqrt{\frac{\kappa_f}{\pi}} y^{-3/2} e^{-\kappa_f/y}, F_Y(y) = \text{erfc}\left(\sqrt{\frac{\kappa_f}{y}}\right) \tag{5}$$

where $\kappa_f \triangleq \eta_f^2 \pi^3 Q_f (\mathbf{E}[\Psi^{1/2}])^2/4$.

Proof: See Appendix II. ■

Remark 1 (Femtocell size): Increasing femtocell size (R_f) *strictly increases* the outage probabilities arising from the femtocell CCI $I_{f,f}$ and $I_{c,f}$ in a two-tier network. To elucidate this, observe that an increase in R_f causes κ_f to increase by a factor R_f^β. By monotonicity of $\text{erfc}(\cdot)$, the cdf's $F_{I_{f,f}}(\cdot), F_{I_{c,f}}(\cdot)$ decrease as κ_f increases, causing a higher outage probability per tier. Intuitively, a femtocell user located on the edge of a femtocell will cause excessive CCI at a nearby femtocell BS; the effect of the CCI appears as a power control penalty factor R_f^β in (5).

Remark 2 (Hopping Protocol): All Tier 2 users within a femtocell are assumed to *jointly* choose a hopping slot. Suppose we compare this against an independent hopping protocol, where users within a femtocell are independently assigned a hopping slot. With independent hopping, the intensity of Φ_f equals $\tilde{\eta}_f = \frac{\lambda_f}{N_{sec}} \cdot (1 - e^{-U_f/N_{hop}})$ (note the difference from η_f in Lemma 1) and the average number of interfering users in an actively transmitting femtocell equals $\frac{U_f/N_{hop}}{1-e^{-U_f/N_{hop}}}$. With an outage threshold of $P_r^f G/(N_{hop}\gamma)$ (3) at a femtocell BS, two observations are in order:

TH-CDMA transmission: When $\frac{G}{N_{hop}} \gg 1$, joint hopping is preferable from an outage probability perspective. Intuitively, joint hopping reduces λ_f by a factor N_{hop}, causing a quadratic decrease in κ_f in (5); independent hopping decreases the number of interfering users per active femtocell, causing a sub-quadratic decrease in $\mathbb{E}[\Psi^{1/2}]^2$. The consequence is that joint hopping results in a greater decrease in $\mathbb{P}_{out}^f$. Using $N_{hop} = 2$, Fig. 3 confirms this intuition; notably, the gap in outage performance is dictated by the hotspot user density: In *heavily loaded femtocells* ($U_f \gg 1$), a joint hopping scheme is clearly superior. For *lightly loaded femtocells*, $\eta_f \simeq \tilde{\eta}_f \approx \frac{\lambda_f U_f}{N_{sec} \cdot N_{hop}}$, implying that independent and joint hopping schemes perform nearly identical.

Random Access transmission: When $N_{hop} = G \gg 1$, the femtocell outage threshold is P_r^f/γ; by consequence, it is preferable to use independent hopping across the tier 2 network.

With joint hopping, even a *single interferer* within a femtocell can cause outage for the user of interest as there is no interference averaging (see Fig. 3); an independent hopping scheme offers increased interference avoidance since the likelihood of two femtocell users sharing a hopping slot is negligible. Consequently, in non-CDMA two-tier cellular networks employing interference avoidance, *independent* assignment of hopping slots is preferable from an outage viewpoint. Using Theorem 1, the macrocellular outage probability is now formulated.

Theorem 2 (Macrocell outage probability): Let outdoor path-loss exponent $\alpha = 4$. *With Poisson in-cell macrocell CCI* $I_{c,in}$, *Gaussian out-of-cell CCI* $I_{c,out}$ *and Lévy-stable femtocell CCI* $I_{c,f}$ *given by* (5)*, the outage probability at the macrocell BS antenna sector is given as:*

$$\epsilon \geq \mathbb{P}_{out}^{c} = 1 - \frac{1}{1 - e^{-\eta_c |\mathcal{H}|}} \sum_{m=1}^{\lfloor \rho_c / P_r^c \rfloor} \frac{e^{-\eta_c |\mathcal{H}|} (\eta_c |\mathcal{H}|)^m}{m!} G_c(\tilde{\rho}_c) \tag{6}$$

where $\eta_c = \frac{\lambda_c}{N_{hop} \cdot N_{sec}}$, $\rho_c = \frac{P_r^c G}{N_{hop} \cdot \gamma}$, $\tilde{\rho}_c = \rho_c - (m-1) P_r^c$ *and* $G_c(t) \triangleq \int_0^t f_{I_{c,out}}(t-y) F_{I_{c,f}}(y) dy$.

Proof: See Appendix III. ■

Theorems 1 and 2 provide the tools to quantify the largest N_f that can be accommodated at a given N_c subject to an outage constraint ϵ. The next step is to compute the outage probability at a femtocell as defined in (3). To do so, assume that the femtocell is located on the axis at a distance R_0 from the macrocell center and the receive antenna at the femtocell BS is aligned at angle θ w.r.t the hexagonal axis (Fig. 2). The following theorem derives a lower bound on the statistics of the tier 1 CCI $I_{f,c}$ at any femtocell located along the hexagonal axis.

Theorem 3 (Lower bound on Macrocellular CCI): At any femtocell BS antenna sector located at distance $0 < R_0 \leq R_c$ *from the macrocell BS along the hexagonal axis:*

1) *The ccdf of the macrocellular interference* $I_{f,c}$ *over a femtocell BS antenna sector is lower bounded as* $\bar{F}_{I_{f,c}}(y) \geq 1 - F_{I_{f,c}}^{lb}(y)$, *where:*

$$F_{I_{f,c}}^{lb}(y) = \exp\left\{ -\frac{\lambda_c}{N_{hop}} \iint_{\mathcal{H}_{sec}} S(r, \phi; y) r dr d\phi \right\} \tag{7}$$

where $S(r, \phi; y) \triangleq \bar{F}_{\Psi}[y / P_r^c \cdot (r / |re^{i\phi} + R_0|)^{\alpha}]$, $\bar{F}_{\Psi}$ *is the ccdf of* $\Psi : 10 \log_{10} \Psi \sim \mathcal{N}(0, 2\sigma_{dB}^2)$, θ *is the femtocell BS antenna alignment angle and* $\mathcal{H}_{sec} \subseteq \mathcal{H}$ *denotes the region inside the reference macrocell enclosed between* $\theta \leq \phi \leq \theta + 2\pi / N_{sec}$.

2) For a corner femtocell $R_0 = R_c$ with an omnidirectional femtocell antenna $N_{sec} = 1$, the ccdf of $I_{f,c}$ is lower bounded as $\bar{F}_{I_{f,c}}(y) \geq 1 - F^{lb}_{I_{f,c}}(y)$, where :

$$F^{lb}_{I_{f,c}}(y) = \exp\left\{-3\frac{\lambda_c}{N_{hop}} \iint_{\mathcal{H}} S(r,\phi;y) r dr d\phi\right\} \tag{8}$$

Proof: See Appendix IV. ■

For a path-loss only model, the lower bounds on the femtocell outage probability can be derived analogously as stated in the following corollary.

Corollary 1: With the above definitions, assuming a pure path-loss model (no shadowing), (7) *and* (8) *hold with* $S(r,\phi;y) \triangleq \mathbf{1}[P^c_r \cdot (|re^{i\phi} + R_0|/r)^{\alpha} \geq y]$

Theorem 3 characterizes the relationship between the intensity of macrocell users and the femtocell outage probability. Observe that the outage probability $\bar{F}^{lb}_{I_{f,c}} \to 1$ *exponentially*, as $\lambda_c \to \infty$. Further, increasing N_{hop} "thins" the intensity of Π_c, thereby mitigating cross-tier CCI at the femtocell BS. Fig. 4 depicts the outage lower bounds to evaluate the impact of macrocellular CCI $I_{f,c}$. Corresponding to an interior and corner femtocell location, the lower bounds are computed when the femtocell BS antenna is either sectored– $N_{sec} = 3$ with antenna alignment angle $\theta = 2\pi/3$ – or omnidirectional. No hopping is used ($N_{hop} = 1$), while a unity power ratio ($P^f_r/P^c_r = 1$) is maintained. Two observations are in order:

Tightness of lower bound: The tightness of (7) and (8) shows that the cross-tier CCI $I_{f,c}$ is primarily impacted by the set of *dominant macrocellular interferers* (13). The implication is that one can perform accurate outage analysis at a femtocell by considering only the *nearest tier 1 users* that individually cause outage. This agrees with the observations in [19], [20].

Infeasibility of omnidirectional femtocells: The benefits of sectored antennas for CCI mitigation at the femtocell BS are evident; with a sectored BS antenna, a corner femtocell (worst-case macrocell CCI) performs considerably better than an interior omnidirectional femtocell.

Using Theorems 1 and 3, the femtocell outage probability (3) is stated in the next theorem.

Theorem 4 (Femtocell outage probability): Let outdoor path-loss exponent $\alpha = 4$. For small λ_c, the femtocell outage probability $\mathbb{P}^f_{out}$ is lower bounded as:

$$\epsilon \geq \mathbb{P}^{f,lb}_{out} \approx 1 - \frac{e^{-U_{f,sec}}}{1 - e^{-U_{f,sec}}} \sum_{m=1}^{\lfloor \rho_f / P^f_r \rfloor} \frac{U^m_{f,sec}}{m!} \cdot G_f(\tilde{\rho}_f) \tag{9}$$

where $U_{f,sec} \triangleq \frac{U_f}{N_{sec}}, \rho_f \triangleq \frac{G P^f_r}{N_{hop} \cdot \gamma}$, $\tilde{\rho}_f = \rho_f - (m-1) \cdot P^f_r$ *and* $G_f(t) \triangleq F_{I_{f,f}}(t) + \int_0^t f_{I_{f,f}}(t - y) \ln(F^{lb}_{I_{f,c}}(y)) dy$.

Proof: See Appendix V. ■

For a *given* N_f, Theorem 4 computes the *largest* N_c which ensures the SIR threshold γ is satisfies for a fraction $(1-\epsilon)$ of the time. Furthermore, the lower bound $F^{lb}_{I_{f,c}}(\cdot)$ was shown to be tight, hence the computed N_c is not overly optimistic. Using Theorems 2 and 4, the OCs for the two-tier network with interference avoidance can now be readily obtained. The following section studies using a femtocell exclusion region around the macrocell BS and a tier selection based femtocell handoff policy, in addition to the interference avoidance strategies discussed hitherto.

IV. Femtocell exclusion region and Tier Selection

Suppose the reference macrocell BS has a femtocell exclusion region $\mathcal{R}^{exc}_f \subset \mathcal{H}$ surrounding it. This idea is motivated by the need to silence neighboring femtocell transmissions which are strong enough to individually cause outage at a macrocell BS; similar schemes have been proposed in [21] and adopted in the CSMA scheduler in the 802.11 standard. The tier 2 femtocell network then forms a heterogeneous SPPP on $\mathcal{H}$ with the average number of femtocells in each cell-site equaling $\lambda_f \cdot (|\mathcal{H}| - |\mathcal{R}^{exc}_f|)$. The following theorem derives a lower bound on the ccdf of the cross-tier femtocell interference $I_{c,f}$ considering the effect of a femtocell exclusion region.

Lemma 2 (Femtocell exclusion region): With a femtocell exclusion region of radius R^{exc}_f around the reference macrocell BS, the ccdf of cross-tier femtocell CCI $I_{c,f}$ is lower bounded as:

$$\bar{F}_{I_{c,f}}(y) \geq 1 - e^{-\pi \eta_f H(y)} \tag{10}$$

where $\delta = \frac{2}{\alpha}$, $u = y \cdot \frac{(R^{exc}_f)^{2/\delta}}{Q_f}$, $H(y) \triangleq (\frac{Q_f}{y})^\delta (\mathbf{E}[\Psi^\delta] - F_\Psi(u)\mathbf{E}[\Psi^\delta \mid \Psi \leq u]) - \bar{F}_\Psi(u)(R^{exc}_f)^2$, $\Psi \triangleq \sum_{i=1}^{U} \Psi_i$, $10\log_{10}\Psi_i \sim \mathcal{N}(0, 2\sigma^2_{dB})$ and $U \sim X|X \geq 1, X \sim \mathrm{Poisson}(U_f)$.

Proof: See Appendix VI. ■

Fig. 5 depicts the macrocell outage performance as a function of the femtocell exclusion radius, assuming $N_c = 1, P^f_r/P^c_r = 1$. Notice that even a small exclusion radius R^{exc}_f results in a significant decrease in $\mathbb{P}^c_{out}$. The implication is that a femtocell exclusion region can increase the number of simultaneous active femtocell transmissions, while satisfying the macrocell outage constraint $\mathbb{P}^c_{out} \leq \epsilon$. Once again, the close agreement between analysis and simulation shows that only the nearby dominant femtocell interferers influence outage events at the macrocell BS.

Corollary 2: With no femtocell exclusion ($R^{exc}_f = 0$), the ccdf of the cross-tier femtocell CCI $I_{c,f}$ at a macrocell is lower bounded as $\bar{F}_{I_{c,f}}(y) \geq 1 - e^{-\pi \eta_f Q_f^\delta \mathbf{E}[\Psi^\delta] y^{-\delta}}$.

Corollary 2 is the two-tier cellular network equivalent of Theorem 3 in Weber *et al.* [20], which derives a lower bound on the outage probability for ad hoc networks with randomized transmission and power control. Finally, this paper considers the influence of a femtocell tier selection based handoff policy wherein any tier 1 macrocellular user within the radius R_f of a femtocell BS undergoes handoff to the femtocell. In essence, the CCI caused by the nearest macrocell users is mitigated, as these users now employ power control to the femtocell BS.

Lemma 3: With a tier selection policy in which any user within a radius R_f of a femtocell undergoes handoff to the femtocell BS, the intensity of tier 1 users within $\mathcal{H}$ after handoff is given as $\lambda_c^{TS}(r) = \lambda_c \cdot e^{-\lambda_f \pi {R_f}^2}$ whenever $r > R_f^{exc}$, where R_f^{exc} is the femtocell exclusion radius.

Proof: See Appendix VII. ■

Remark 3: For small λ_f and $r > R_f^{exc}$, a first-order Taylor approximation shows that $\lambda_c^{TS} \approx \lambda_c \cdot (1 - \lambda_f \pi R_f^2)$. The interpretation is that tier-selection offers marginal benefits for small femtocell sizes ($R_f \ll R_c$). Intuitively, a small sized femtocell does not cover "enough space" for significant numbers of macrocellular users in Ω_c to accomplish femtocell handoff. However, Theorem 1 shows that a small femtocell size does lead to a lower uplink outage probability.

Remark 4: The network OCs considering the effects of a femtocell exclusion region and tier selection can be obtained by applying Lemmas 2 and 3 in Theorems 2 and 4 respectively. In doing so, we approximate $I_{f,f}$ as a Poisson SNP whose cdf is described by (1).

V. Numerical Results

System parameters are given in Table I, and the LabVIEW environment was used for numerical simulations. The setup consists of the region $\mathcal{H}$ surrounded by 18 macrocell sites to consider two rings of interferers and $2\pi/3$ sectored antennas at each BS. In (10), the statistics of the shadowing gain Ψ were empirically estimated using the MATLAB functions `ksdensity` and `ecdf` respectively. The OCs were analytically obtained using Theorems 1-4 for an outage constraint $\epsilon = 0.1$ in (4). The following plots compare the OCs for a shared spectrum network with interference avoidance against a split spectrum network with omnidirectional femtocells.

Figs 6 and 7 plot OCs for a macrocell and interior femtocell for $P_r^f/P_r^c = 1, 10, 100$ and $N_{hop} = 1$. The femtocell uses a sectored receive antenna with $N_{sec} = 3, \theta = 2\pi/3$. The close agreement between the theoretical and empirical OC curves indicates the accuracy of the analysis. Observe that the outage constraints oppose one another: increasing P_r^f/P_r^c *decreases* the largest

N_f sustainable for a given N_c from the macrocell BS perspective. From the femtocell standpoint, increasing P_r^f/P_r^c *increases* the largest N_c which is sustainable for a given N_f.

Figs 8 through 10 plot the performance of the shared spectrum network employing interference avoidance for a corner and an interior femtocell, as a function of N_{hop} and P_r^f/P_r^c. Fig 8 shows that with $P_r^f/P_r^c = 1$ and a lightly loaded tier 1 network, the corner femtocell can achieve *greater than 7x* improvement in N_f relative to the split spectrum network. Intuitively, with $P_r^f/P_r^c = 1$, a macrocell BS tolerates a large cross-tier CCI; the downside being that the femtocell BS experiences higher macrocellular CCI arising from tier 1 users transmitting at maximum power near the cell edge. This explains why N_f decreases rapidly with increasing N_c in the OC curves for a corner femtocell. With $P_r^f/P_r^c = 10$, the OCs for corner and interior femtocells in Figs 9 and 10 offer *greater than 2.5x* improvement in N_f relative to the split spectrum network. Additionally, a greater degree of load balancing is achieved: with an interior femtocell location, a maximum of $N_c = 45$ tier 1 users can be accommodated. The inference is that in a shared spectrum two-tier network, interference avoidance offers considerable improvement in *tier 2 femtocell density* N_f at low N_c; to achieve *load balancing* by increasing N_c at the expense of N_f, an *order wise difference in receive power ratio* is required. We aver that a practical wireless system use a larger P_r^f/P_r^c closer to the corner femtocell relative to the interior; this will ensure that both the interior and corner femtocells can sustain identical number of tier 1 users.

Fig. 11 shows the two-tier OCs when users in each tier employ a femtocell exclusion region and a tier selection policy for femtocell handoff. We observe an increase in N_f by up to 10 additional femtocells (or $10 * U_f = 50$ users) for $N_c < 30$ users. Both femtocell exclusion and tier selection *do not* lead to a higher N_c. The reason is that a femtocell exclusion region does not alleviate tier 1 CCI at a femtocell. Furthermore, an explanation for the conservative gains in N_f is that there is a maximum tolerable interference to sustain the outage requirements at a given femtocell, that prevents a substantial increase in the number of actively transmitting femtocells. Next, owing to small femtocell sizes, a tier selection policy succeeds in curbing tier 1 CCI mainly for a large N_f, which is sustainable when N_c is small (to satisfy $\mathbb{P}_{out}^c \leq \epsilon$). This explains the dominant gains in N_f at a low-to-moderate N_c.

A relevant question is to ask: *"How does the system capacity with randomly placed users and hotspots compare against a two-tier network with a given configuration?"* Due to space limitations, our paper does not address this question directly. We refer the reader to Kishore *et* *al.* [7, Page 1339]. Their results agree with ours' in that there is a decline in the system capacity, because the configuration contains high levels of cross-tier CCI.

Kishore proposes to alleviate cross-tier CCI by varying the macrocell coverage region, through exchanging the pilot channel strength with the microcell. Our model assumes that femtocells (placed by end consumer) operate with *minimal information exchange* with the macrocell BS. Due to reasons of security and scalability–there may be hundreds of embedded femtocells within a densely populated macrocell– handing off unsubscribed users from macrocell to a femtocell hotspot may not be practical. Moreover, femtocell hotspots have a small radio range (< 50 meters). This necessitates an interference avoidance strategy.

VI. Conclusion

This paper has presented an uplink capacity analysis and interference avoidance strategy for a shared spectrum two-tier DS-CDMA network. We derive exact outage probability at a macrocell BS and tight lower bounds on the ccdf of the CCI at a femtocell. Interference avoidance through a TH-CDMA physical layer coupled with sectorized receive antennas is shown to consistently outperform a split spectrum two-tier network with omnidirectional femtocell antennas. Considering the worst-case interference at a corner femtocell, the network OCs show a 7x improvement in femtocell density. Load balancing users in each tier is achievable through a orderwise difference in receive powers in each tier. Additional interference avoidance using a femtocell exclusion region and a tier selection based femtocell handoff offers conservative improvements in the OCs. The message is clear: Interference avoidance strategies can make shared spectrum two-tier networks a viable proposition in practical wireless systems.

Acknowledgement

We acknowledge Dr. Alan Gatherer and Dr. Zukang Shen of Texas Instruments for their valuable input and sponsorship of this research. The contributions of Andrew Hunter are also gratefully acknowledged.

Appendix I

Consider the Poisson field of interferers as seen at any antenna sector (either macrocell or femtocell BS) with antenna alignment angle θ (Fig. 2). Assuming a perfect antenna radiation pattern, the interfering Poisson field forms heterogeneous SPPPs $\hat{\Omega}_c$ and $\hat{\Omega}_f$ with intensities given by,

$$\hat{\lambda}_c(r,\phi) = \frac{\lambda_c}{N_{hop}}\mathbf{1}(\phi \in [\theta, \theta + \frac{2\pi}{N_{sec}}]), \hat{\lambda}_f(r,\phi) = \frac{\lambda_f}{N_{hop}}(1 - e^{-U_f})\mathbf{1}(\phi \in [\theta, \theta + \frac{2\pi}{N_{sec}}]) \quad (11)$$

where $\mathbf{1}(\cdot)$ represents the indicator function. The following observations rigorously explain (11).

Hopping slot selection: The set of macrocell users and femtocell BSs transmitting over any hopping slot is obtained by independent Bernoulli thinning of the SPPPs (Ω_c, Ω_f) by the probability of choosing that hopping slot namely $1/N_{hop}$.

Active femtocell selection: The factor $(1 - e^{-U_f})$ arises because the set of femtocells with *at least one actively transmitting user* is obtained using independent Bernoulli thinning of Ω_f [17]. Observe that a femtocell with $U \geq 1$ actively transmitting users satisfies $\mathbb{E}[U] = \frac{U_f}{1-e^{-U_f}}$. The event consisting of marking femtocells by the probability that they contain at least one actively transmitting user and the event of marking femtocells by the probability of choosing a common hopping slot are independent; this implies that the resulting SPPP $\hat{\Omega}_f$ has intensity $\frac{\lambda_f}{N_{hop}} \cdot (1 - e^{-U_f})$. Finally, using the Mapping theorem [17, Section 2.3] for Poisson processes, one can map the heterogeneous SPPPs $\hat{\Omega}_c$ and $\hat{\Omega}_f$ over one antenna sector to homogeneous SPPPs Φ_c and Φ_f over $\mathbb{R}^2$ with intensities $\eta_c = \frac{\lambda_c}{N_{hop} \cdot N_{sec}}$ and $\eta_f = \frac{\lambda_f}{N_{hop} \cdot N_{sec}} \cdot (1 - e^{-U_f})$ respectively.

APPENDIX II

From (2), $I_{c,f}$ (and $I_{f,f}$) are distributed as a Poisson SNP $\hat{Y} = \sum_{i \in \hat{\Omega}_f} Q_f \Psi_i |X_i|^{-\alpha}$ over an antenna sector of width $2\pi/N_{sec}$. Next, the Mapping theorem [17] is used to prove (5).

1) Invoke Lemma 1 for mapping $\hat{\Omega}_f$ to a homogeneous SPPP Φ_f on $\mathbb{R}^2$. This implies that $\hat{Y}$ is distributed identically as $Y = \sum_{i \in \Phi_f} Q_f \Psi_i |X_i|^{-\alpha}$.

2) Map the planar SPPP defining Φ_f with intensity η_f to a 1D SPPP with intensity $\pi\eta_f$ using Proposition 1, Theorem 2 in [16]. For doing so, rewrite Y as, $Y = \sum_{i \in \Phi_f} Q_f \Psi_i (|X_i|^2)^{-\alpha/2}$ which represents a SPPP on the line with Poisson arrival times $|X_i|^2$ and intensity $\pi\eta_f = \frac{\pi\lambda_f}{N_{hop} \cdot N_{sec}}(1 - e^{-U_f})$.

Consequently, Y is identically distributed as a 1D SPPP with intensity $\pi\eta_f$, which represents a Lévy-stable distribution with stability exponent $\delta = 2/\alpha$ [22], and a characteristic function given by $Q_Y(s) = \exp\left[-\pi\eta_f\Gamma(1-\delta)\mathbf{E}[\Psi^\delta](Q_f s)^\delta\right]$, where $\Gamma(z) \triangleq \int_0^\infty t^{z-1}e^{-t}dt$ is the gamma function. In particular, when $\alpha = 4$, Y follows a Lévy-stable distribution with stability exponent $\delta = 0.5$, with statistics (5) obtained from Equation (30) in [15].

Appendix III

At the macrocell BS, the interference denoted by $I_{c,in}, I_{c,out}$ and $I_{c,f}$ are mutually independent random variables. The macrocell outage probability $\mathbb{P}^c_{out}$ defined in (3) can be computed by the probability of the complementary event, corresponding to the probability that the cumulative interference does not exceed the SIR threshold $\rho_c = P^c_r G/(N_{hop} \cdot \gamma)$. The cdf of $(I_{c,in} + I_{c,out} + I_{c,f})$ can be computed using a three-fold convolution. Observe that the event that the intra-tier macrocell CCI from $(k-1)$ in-cell tier 1 interferers $I_{c,in}$ equals $(k-1) \cdot P^c_r$ given at least one active tier 1 user (user of interest) is equivalent to the event that Φ_c (Lemma 1) has k elements within $\mathcal{H}$. The probability of this event is given by,

$$\Pr[I_{c,in} = (k-1) \cdot P^c_r \mid k \geq 1] = \Pr[|\Phi_c| = k \mid |\Phi_c| \geq 1] = \frac{1}{1 - e^{-\eta_c|\mathcal{H}|}} \frac{e^{-\eta_c|\mathcal{H}|}(\eta_c|\mathcal{H}|)^k}{k!} \quad (12)$$

The total interference caused by the $(k-1)$ interfering macrocell users equals $(k-1) \cdot P^c_r$; there is no outage if the residual interference $I_{c,out} + I_{c,f}$ is less than $\rho_c - (k-1) \cdot P^c_r$. Using independence of $I_{c,out}$ and $I_{c,f}$, Theorem 1 and Gaussian distributed $I_{c,out}$, the result follows.

Appendix IV

The interference experienced at a femtocell BS antenna sector $\theta \leq \phi \leq \theta + 2\pi/N_{sec}$ is lower bounded by the macrocellular CCI arising within $\mathcal{H}_{sec}$. If the femtocell BS is located at distance R_0 from the reference macrocell, then any macrocell user located at polar coordinates (r, ϕ) w.r.t the femtocell BS causes an interference equaling $P^c_r(|R_0 + re^{i\phi}|/r)^\alpha$ at the femtocell BS. Corresponding to the heterogeneous SPPP Π_c (see Definition 3), outage events at the femtocell BS arising from macrocellular CCI $I_{f,c}$ can be categorized into two types: In the first type, outage events arise due to CCI caused by a single user in Π_c. The second class of outage events occur due to the macrocell interferers whose *cumulative* CCI causes outage [19]. This class precludes all interferers falling in the first category. Mathematically, for an outage threshold y at the femtocell BS, split Π_c into two disjoint heterogeneous Poisson SPPPs $\Pi_c = \Pi_{c,y} \cup \Pi^C_{c,y}$ corresponding to the set of *dominant* and *non-dominant* macrocellular interferers:

$$\Pi_{c,y} \triangleq \{(r_i, \phi_i) \in \Pi_c : P^c_r \Psi_i(|r_i e^{i\phi_i} + R_0|/r_i)^\alpha \geq y\}, \Pi^C_{c,y} = \Pi_c \setminus \Pi_{c,y} \quad (13)$$

At any point $(r, \phi) \in \mathcal{H}$, the intensity of $\Pi_{c,y}$ denoted by $\lambda_{c,y}(r, \phi)$ is given as,

$$\lambda_{c,y}(r, \phi) = \frac{\lambda_c}{N_{hop}} \bar{F}_\Psi \left[\frac{yr^\alpha}{P^c_r |re^{i\phi} + R_0|^\alpha} \right] \cdot \mathbf{1}[\theta \leq \phi \leq \theta + 2\pi/N_{sec}] \quad (14)$$

In the event of $\Pi_{c,y}$ being non empty, the femtocell BS experiences outage, arising from the CCI caused by a user in $\Pi_{c,y}$. Therefore, $\mathbb{P}_{out}^{f}$ is lower bounded by the probability that $\Pi_{c,y}$ has at least one element. Equation (7) results from the Poisson void probability of the complementary event namely $\Pr\left(|\Pi_{c,y}| = 0\right)$ [17]. This completes the proof for the first assertion.

To prove (8), recognize that a corner femtocell with an omnidirectional BS antenna encounters macrocellular CCI from the three surrounding cellsites. The dominant macrocell interferer set $\Pi_{c,y}$ can be expressed as $\Pi_{c,y} = \bigcup_{i=1}^{3} \Pi_{c,y}^{i}$, where $\Pi_{c,y}^{i}$ denotes the dominant macrocell interferer set in neighboring cellsite i. The heterogeneous SPPPs $\Pi_{c,y}^{i}$ are non-intersecting with an intensity expressed by (14). The ccdf of $I_{f,c}$ is then lower bounded by the probability of $\Pi_{c,y}$ being non empty, which can be deduced from the event that $\Pi_{c,y}^{i}, i = 1 \cdots 3$ are empty.

$$F_{I_{f,c}}^{lb}(y) = \prod_{i=1}^{3} \Pr\left(|\Pi_{c,y}^{i}| = 0\right) = \exp\left\{-3\frac{\lambda_c}{N_{hop}} \iint_{\mathcal{H}} S(r,\phi;y) r dr d\phi\right\} \tag{15}$$

To complete the proof, use pairwise independence of the events that $\Pi_{c,y}^{i}$ and $\Pi_{c,y}^{j}$ are empty and $S(r,\phi;y)$ in (7) to show that $\bar{F}_{I_{f,c}}(\cdot)$ is lower bounded as $\bar{F}_{I_{f,c}}(y) \geq 1 - F_{I_{f,c}}^{lb}(y)$ in (15).

Appendix V

The number of femtocell users within a femtocell BS antenna sector is Poisson distributed with mean U_f/N_{sec}. The overall CCI is composed of three terms namely $I_{f,in}, I_{f,f}$ and $I_{f,c}$ which are mutually independent. Given m actively transmitting femtocell users including the user of interest, $I_{f,in} = (m-1) \cdot P_r^f$; consequently, the outage threshold for $I_{f,f} + I_{f,c}$ equals $\tilde{\rho}_f = \rho_f - (m-1) \cdot P_r^f, \rho_f \triangleq G P_r^f / (N_{hop} \cdot \gamma)$ using (3). A lower bound on $\mathbb{P}_{out}^{f}$ is obtained as,

$$\epsilon \geq \mathbb{P}_{out}^{f,lb} = 1 - \frac{e^{-U_{f,sec}}}{1 - e^{-U_{f,sec}}} \sum_{m=1}^{\lfloor \rho_f / P_r^f \rfloor} \frac{U_{f,sec}^{m}}{m!} \cdot F_{I_{f,c}^{lb} + I_{f,f}}(\tilde{\rho}_f) \tag{16}$$

$$= 1 - \frac{e^{-U_{f,sec}}}{1 - e^{-U_{f,sec}}} \sum_{m=1}^{\lfloor \rho_f / P_r^f \rfloor} \frac{U_{f,sec}^{m}}{m!} \cdot [F_{I_{f,c}}^{lb} * f_{I_{f,f}}](\tilde{\rho}_f) \tag{17}$$

$$\approx 1 - \frac{e^{-U_{f,sec}}}{1 - e^{-U_{f,sec}}} \sum_{m=1}^{\lfloor \rho_f / P_r^f \rfloor} \frac{U_{f,sec}^{m}}{m!} \cdot [(1 + \ln(F_{I_{f,c}}^{lb})) * f_{I_{f,f}}](\tilde{\rho}_f) \tag{18}$$

$$= 1 - \frac{e^{-U_{f,sec}}}{1 - e^{-U_{f,sec}}} \sum_{m=1}^{\lfloor \rho_f / P_r^f \rfloor} \frac{U_{f,sec}^{m}}{m!} \cdot G_f(\tilde{\rho}_f) \tag{19}$$

Equation (16) uses the lower bound on macrocell CCI $I_{f,c}^{lb}$ arising from the set of dominant macrocell interferers (13). (17) uses pairwise independence of $I_{f,f}$ and $I_{f,c}$ for performing a convolution of the respective probabilities. Finally, (18) follows from a first-order Taylor series approximation of $F_{I_{f,c}}^{lb}$ in (7) using $e^x \approx (1+x)$ for small λ_c in the low outage regime.

APPENDIX VI

For an outage threshold y, the SPPP $\hat{\Omega}_f$ comprising the tier 2 femtocell CCI can be split into the set of dominant and non-dominant femtocells denoted by $(\hat{\Omega}_{f,y}, \hat{\Omega}_{f,y}^C)$ respectively. The heterogeneous SPPP $\hat{\Omega}_{f,y} = \{(r_i,\phi_i) \in \hat{\Omega}_f : Q_f \Psi_i r_i^{-\alpha} \geq y\}$ consists of actively transmitting femtocells which are capable of individually causing outage at a macrocell BS. At any (r,ϕ) w.r.t macrocell BS, the intensity of $\hat{\Omega}_{f,y}$ is given by $\hat{\lambda}_{f,y}(r,\phi) = \hat{\lambda}_f(r,\phi)\cdot \bar{F}_\Psi(yr^\alpha/Q_f)$. The ccdf of the femtocell CCI $I_{f,c}$ is lower bounded by the probability that the set $\hat{\Omega}_{f,y}$ is non-empty. For if $\hat{\Omega}_{f,y}$ contains at least one element, then the macrocell BS antenna sector is in outage (by construction of $\hat{\Omega}_{f,y}$). Using the void probability of $\hat{\Omega}_{f,y}$, the lower bound is given as:

$$\bar{F}_{I_{c,f}}(y) \geq \bar{F}_{I_{c,f}}^{lb}(y) = 1 - \exp\left\{-\frac{2\pi\lambda_f}{(N_{hop}\cdot N_{sec})}\int_{R_f^{exc}}^{\infty} \bar{F}_\Psi\left(\frac{yr^\alpha}{Q_f}\right)dr\right\} \tag{20}$$

$$= 1 - \exp\left\{-\pi\eta_f Q_f^\delta y^{-\delta}\int_u^\infty \bar{F}_\Psi(t)d(t^\delta)\right\} \tag{21}$$

$$= 1 - \exp\left\{-\pi\eta_f Q_f^\delta y^{-\delta}\left[\int_u^\infty t^\delta f_\Psi(t)dt - \bar{F}_\Psi(u)(R_f^{exc})^2\right]\right\} \tag{22}$$

Equation (21) follows by substituting $t = yr^\alpha/Q_f$ in (20), while (22) is obtained using integration by parts. Using $\int_u^\infty t^\delta f_\Psi(t)dt = \mathbf{E}[\Psi^\delta] - F_\Psi(u)\mathbf{E}[\Psi^\delta \mid \Psi \leq u]$ in (22) completes the proof.

APPENDIX VII

In the region $0 \leq r \leq R_f^{exc}$ around the reference macrocell, actively transmitting femtocells are absent, so that there are no femtocells for handoff to occur for any user in Ω_c. Consequently, the intensity of the tier 1 macrocellular users in $0 < r < R_f^{exc}$ equals λ_c. For $r > R_f^{exc}$, the intensity of the macrocell users is found by computing the probability that any point in Ω_c (prior tier selection) does not fall within R_f meters of a femtocell BS. This is equivalent to computing the void probability of Ω_f within a circle of radius R_f of every point in Ω_c, which equals $e^{-\lambda_f \pi R_f^2}$.

This paper assumes an *independent* Bernoulli thinning of each point in Ω_c by the probability that a tier 1 user falls with R_f of a femtocell. Strictly speaking, this statement is not correct: Given two closely spaced tier 1 users in Ω_c, the event that the first user undergoes femtocell handoff is correlated with a nearby user in Ω_c undergoing handoff with the same femtocell. However, we justify that this assumption is reasonable while considering the small size of each femtocell. Then, the intensity of tier 1 users following the femtocell handoff is obtained by iid Bernoulli thinning of Ω_c by the void probability $e^{-\lambda_f \pi R_f^2}$ [17], which completes the proof.

TABLE I

SYSTEM PARAMETERS

Symbol	**Description**	**Value**
$\mathcal{H}$	Region inside reference cellsite	N/A
Ω_c, Ω_f	SPPPs defining Tier 1, Tier 2 users	N/A
R_c, R_f	Macro/Femtocell Radius	$500, 20$ meters
U_f	Poisson mean users per femtocell	5
N_{sec}	Macrocell/Femtocell BS antenna sectors	3
N_{hop}	CDMA Hopping slots	$1, 2, 4$
α, β	Path-loss exponents	$4, 2$
G	Processing Gain	128
γ	Target SIR per tier	2 [C/I=3 dB]
ϵ	Target Outage Probability	0.1
σ_{dB}	Lognormal shadowing parameter	4 dB
P_r^c	Macrocell receive power	1
P_r^f	Femtocell receive power	1,10,100
d_{0c}, d_{0f}	Reference distances	$100, 5$ meters
f_c	Carrier Frequency	2 GHz

REFERENCES

[1] J. Shapira, “Microcell engineering in CDMA cellular networks,” *IEEE Transactions on Vehicular Technology*, vol. 43, no. 4, pp. 817–825, Nov. 1994.

[2] A. Doufexi, E. Tameh, A. Nix, S. Armour, and A. Molina, “Hotspot wireless LANs to enhance the performance of 3G and beyond cellular networks,” *IEEE Communications Magazine*, vol. 41, no. 7, pp. 58–65, July 2003.

[3] A. Ganz, C. M. Krishna, D. Tang, and Z. J. Haas, “On optimal design of multitier wireless cellular systems,” *IEEE Communications Magazine*, vol. 35, no. 2, pp. 88–93, Feb. 1997.

[4] S. Kishore, L. J. Greenstein, H. V. Poor, and S. C. Schwartz, “Downlink user capacity in a CDMA macrocell with a hotspot microcell,” in *Proc., IEEE Global Telecommunications Conference*, vol. 3, Dec. 2003, pp. 1573–1577.

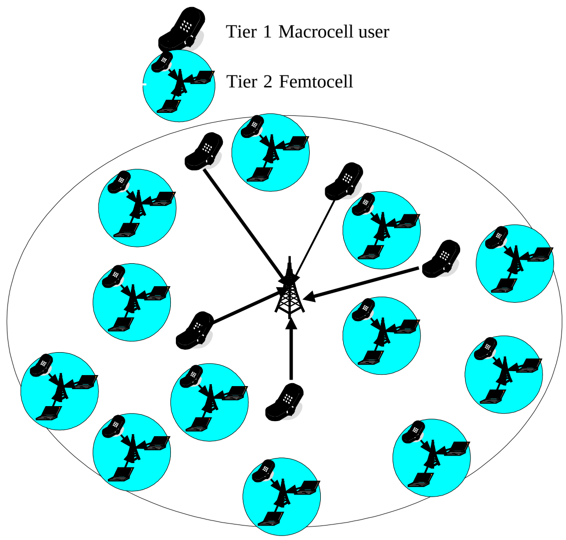

Fig. 1. A Two-tier Femtocell network with DS-CDMA Transmission

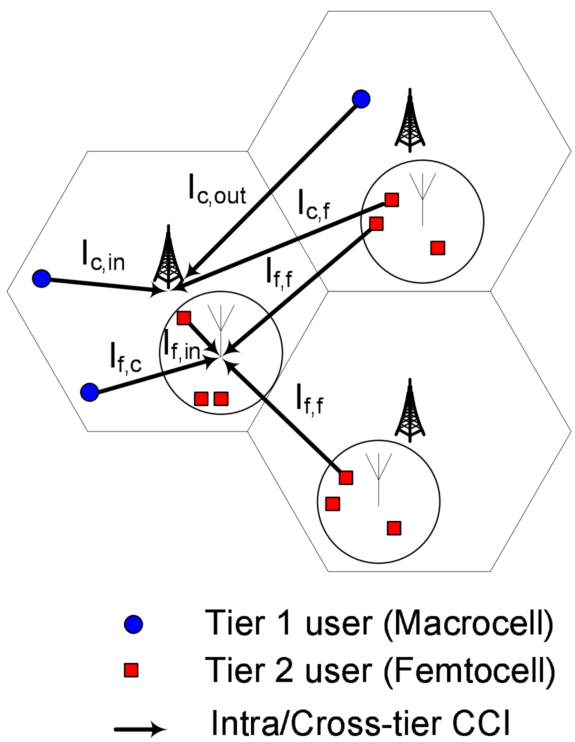

Fig. 2. Intra- and cross-tier CCI at each tier. The arrows denote the CCI arising from either a Tier 1 or Tier 2 user.

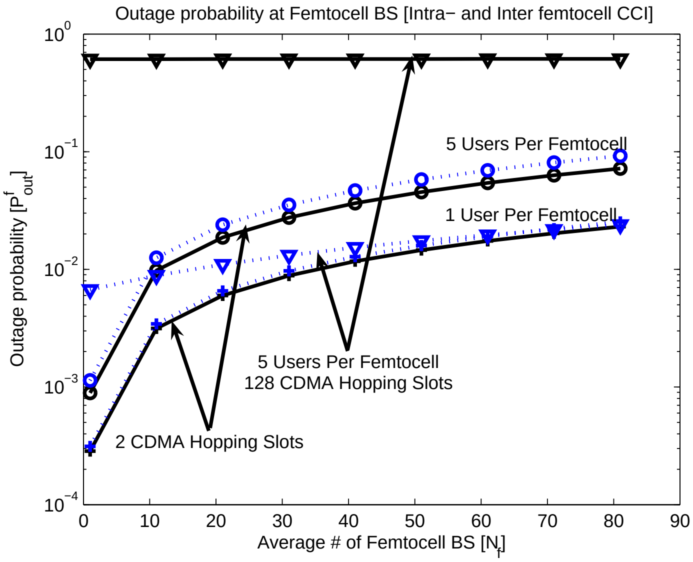

Fig. 3. Comparison of Joint and Independent Hopping protocols at a femtocell BS with Antenna Sectoring. Solid lines represent the joint hopping performance when all users within a femtocell share a common hopping slot. Dotted lines indicate the performance when every femtocell user is assigned an independent CDMA hopping slot.

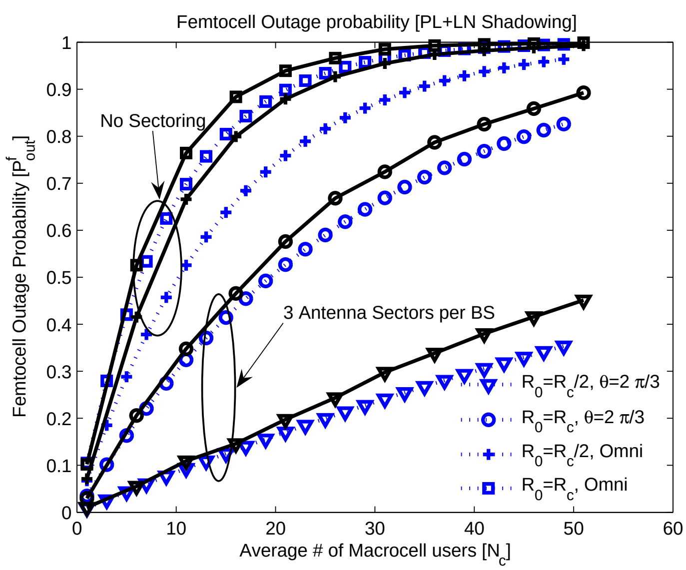

Fig. 4. Outage Lower Bounds for Interior and Corner Femtocell ($N_{hop} = 1, P_r^f = P_r^c$). Blue dotted lines indicate theoretical bounds and black solid lines indicate empirically estimated probabilities.

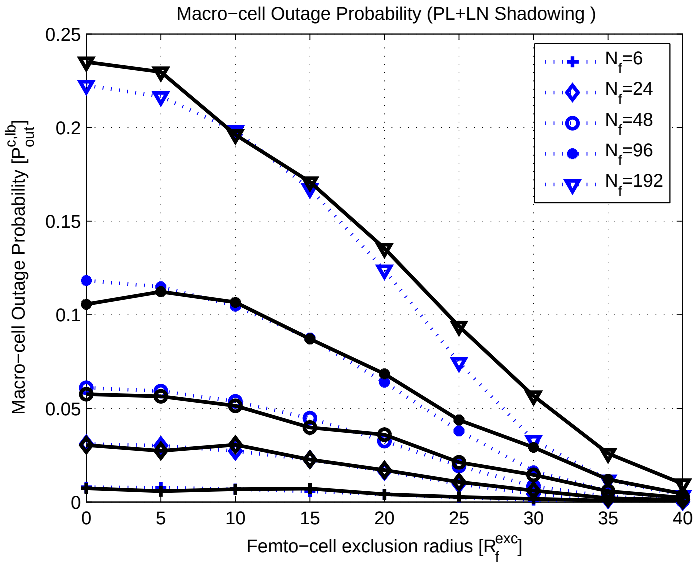

Fig. 5. Macrocell Outage Performance with Femtocell exclusion, $N_c = 24, P_r^f = P_r^c$. Blue dotted lines indicate theoretical bounds and black solid lines indicate empirically estimated probabilities.

[5] S. Kishore, L. Greenstein, H. Poor, and S. Schwartz, “Uplink user capacity in a CDMA macrocell with a hotspot microcell: Exact and approximate analyses,” *IEEE Transactions on Wireless Communications*, vol. 2, no. 2, pp. 364–374, Mar. 2003.

[6] ——, “Uplink user capacity in a multicell CDMA system with hotspot microcells,” *IEEE Transactions on Wireless Communications*, vol. 5, no. 6, pp. 1333–1342, June 2006.

[7] S. Kishore, L. J. Greenstein, H. V. Poor, and S. C. Schwartz, “Uplink user capacity in a CDMA system with hotspot microcells: effects of Finite Transmit power and Dispersion,” *IEEE Transactions on Wireless Communications*, vol. 5, no. 2, pp. 417–426, Feb. 2006.

[8] D. H. Kim, D. D. Lee, H. J. Kim, and K. C. Whang, “Capacity analysis of macro/microcellular CDMA with power ratio control and tilted antenna,” *IEEE Transactions on Vehicular Technology*, vol. 49, no. 1, pp. 34–42, Jan. 2000.

[9] J.-S. Wu, J.-K. Chung, and M.-T. Sze, “Analysis of uplink and downlink capacities for two-tier cellular system,” *IEE Proceedings- Communications*, vol. 144, no. 6, pp. 405–411, Dec. 1997.

[10] R. S. Karlsson, “Radio resource sharing and capacity of some multiple access methods in hierarchical cell structures,” in *Proc., IEEE Vehicular Technology Conference*, vol. 5, Amsterdam, Sept. 1999, pp. 2825–2829.

[11] D. Joseph, B. Manoj, and C. Siva Ram Murthy, “The interoperability of Wi-Fi hotspots and packet cellular networks and the impact of user behaviour,” in *Proc., IEEE International Symposium on Personal, Indoor and Mobile Radio Communications*, vol. 1, Sept. 2004, pp. 88–92.

[12] C.-L. I, L. J. Greenstein, and R. D. Gitlin, “A microcell/macrocell cellular architecture for low- and high-mobility wireless users,” *IEEE Journal on Selected Areas in Communications*, vol. 11, no. 6, pp. 885–891, Aug. 1993.

[13] F. Baccelli. Stochastic geometry: A tool for modeling telecommunication networks. [Online]. Available: `http://www.di.ens.fr/~mistral/sg/`

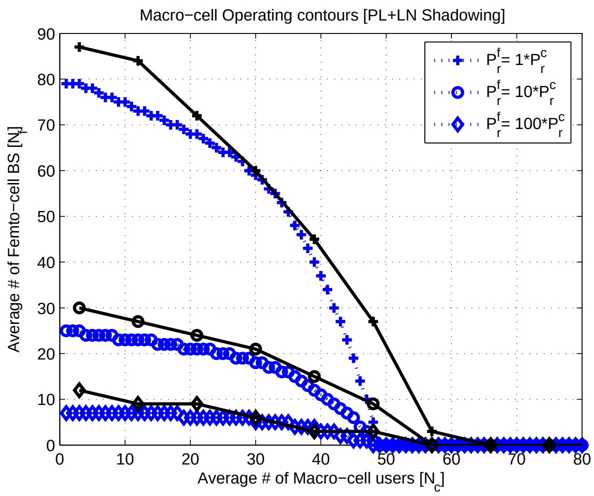

Fig. 6. Macrocell OC (Largest N_c for a given N_f satisfying $\mathbb{P}^c_{out} \leq \epsilon$), $N_{hop} = 1, N_{sec} = 3$

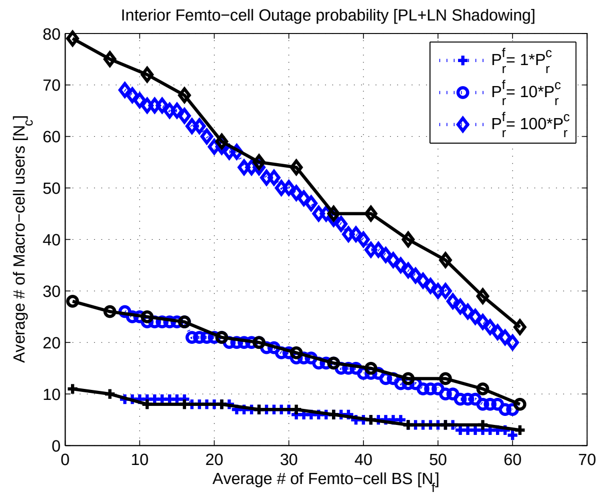

Fig. 7. Interior Femtocell OC (Largest N_f for a given N_c satisfying $\mathbb{P}^f_{out} \leq \epsilon$), $N_{hop} = 1, N_{sec} = 3$

[14] C. C. Chan and S. Hanly, "Calculating the outage probability in a CDMA network with Spatial Poisson traffic," *IEEE Transactions on Vehicular Technology*, vol. 50, no. 1, pp. 183–204, Jan. 2001.

[15] S. Lowen and M. Teich, "Power-law shot noise," *IEEE Transactions on Information Theory*, vol. 36, no. 6, pp. 1302–1318, Nov. 1990.

[16] J. Ilow and D. Hatzinakos, "Analytic alpha-stable noise modeling in a Poisson field of interferers or scatterers," *IEEE Transactions on Signal Processing*, vol. 46, no. 6, pp. 1601–1611, June 1998.

[17] J. Kingman, *Poisson Processes*. Oxford University Press, 1993.

[18] M. G. Jansen and R. Prasad, "Capacity, throughput, and delay analysis of a cellular DS CDMA system with imperfect power control and imperfect sectorization," *IEEE Transactions on Vehicular Technology*, vol. 44, pp. 67–75, Feb. 1995.

[19] S. Weber, X. Yang, J. Andrews, and G. de Veciana, "Transmission capacity of wireless ad hoc networks with outage constraints," *IEEE Transactions on Information Theory*, vol. 51, no. 12, pp. 4091–4102, Dec. 2005.

[20] S. Weber, J. Andrews, and N. Jindal, "The effect of fading, channel inversion, and threshold scheduling on ad hoc networks," *To appear, IEEE Transactions on Information Theory*, Nov. 2007.

[21] A. Hasan and J. G. Andrews, "The guard zone in wireless ad hoc networks," *IEEE Transactions on Wireless Communications*, vol. 6, no. 3, pp. 897–906, Mar. 2007.

[22] G. Samorodnitsky and S. Taqqu, *Stable Non-Gaussian Random Processes*. Chapman and Hall, 1994.

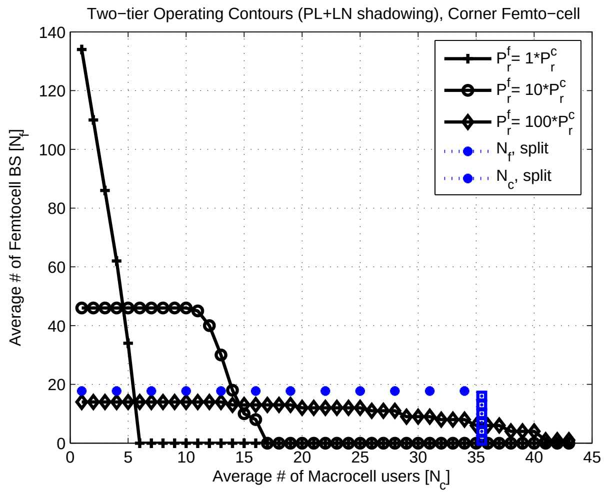

Fig. 8. Network OCs for different macrocell-femtocell received power ratios and fixed hopping slots, Corner femtocell reference ($N_{hop} = 4, N_{sec} = 3$)

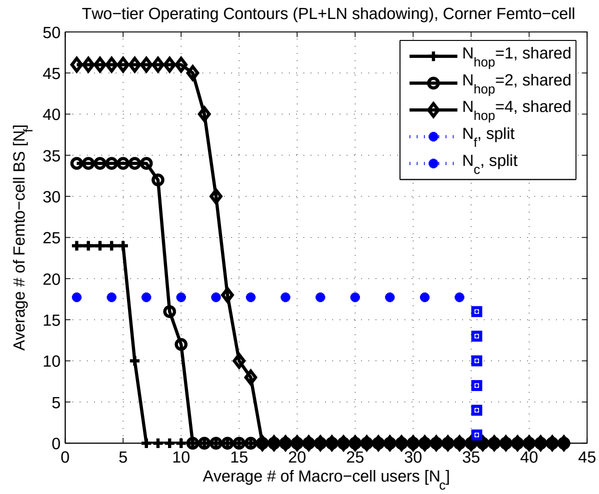

Fig. 9. Network OCs with different hopping slots, Corner femtocell reference, $\frac{P_r^f}{P_r^c} = 10, N_{sec} = 3$

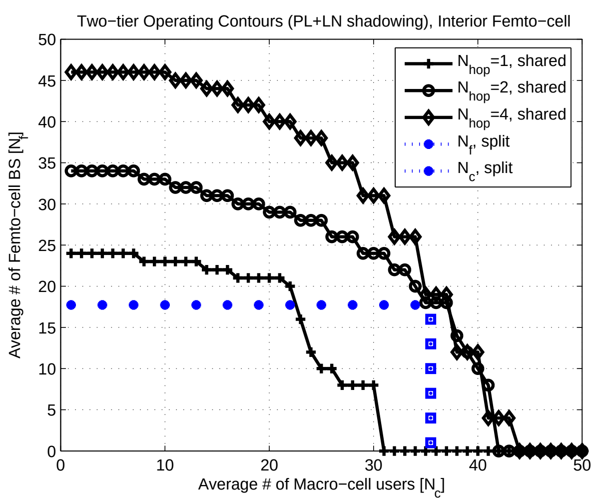

Fig. 10. Network OCs with different hopping slots, Interior femtocell reference, ($\frac{P_r^f}{P_r^c} = 10, N_{sec} = 3$)

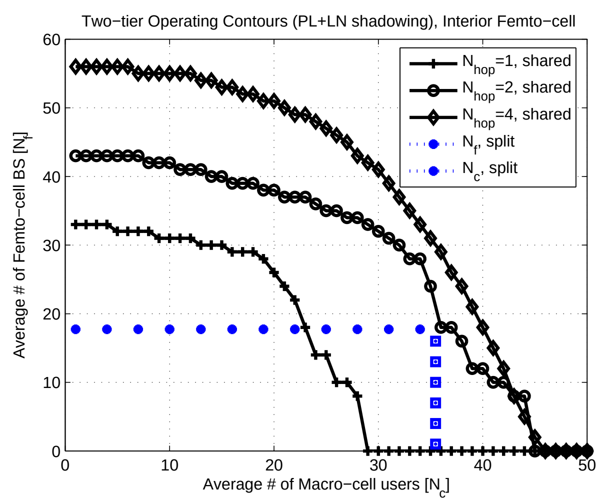

Fig. 11. Network OCs with Tier Selection and Femtocell exclusion, Interior femtocell, $\frac{P_r^f}{P_r^c} = 10, N_{sec} = 3, R_f^{exc} = 20$